

ENHANCING TRUST-REGION BAYESIAN OPTIMIZATION VIA DERIVATIVES OF GAUSSIAN PROCESSES

Anonymous authors

Paper under double-blind review

ABSTRACT

Bayesian Optimization (BO) has been widely applied to optimize expensive black-box functions while retaining sample efficiency. However, scaling BO to high-dimensional spaces remains challenging. Existing literature proposes performing standard BO in several local trust regions (TuRBO) for heterogeneous modeling of the objective function and avoiding over-exploration. Despite its advantages, using local Gaussian Processes (GPs) reduces sampling efficiency compared to a global GP. To enhance sampling efficiency while preserving heterogeneous modeling, we propose to construct several local quadratic models using gradients and Hessians from a global GP, and select new sample points by solving the bound-constrained quadratic program. We provide a convergence analysis and demonstrate through experimental results that our method enhances the efficacy of TuRBO and outperforms a wide range of high-dimensional BO techniques on synthetic functions and real-world applications.

1 INTRODUCTION

Bayesian Optimization (BO) has been one of the popular methods for the global optimization of expensive black-box functions due to its high sampling efficiency. Applications include hyperparameter tuning for deep learning (Hvarfner et al., 2022), discovering new molecules for chemical engineering (Gómez-Bombarelli et al., 2018), searching an optimal policy for reinforcement learning (Müller et al., 2021), and so on. BO is a sequential model-based approach consisting of two main components: a surrogate model and an acquisition function. The surrogate model, typically implemented as a Gaussian Process regression, is used to improve the sampling efficiency of BO by modeling the objective function. The acquisition function is used to determine the next sample point.

While BO performs well in optimizing low-dimensional functions, it struggles with high-dimensional problems for several reasons. First, the surrogate model loses accuracy in the high-dimensional space when estimating the objective function. This is because it is impossible to fill the high-dimensional space with finite sample points, even with a large sample size (Györfi et al., 2002). Second, the computational complexity of optimizing the acquisition function grows exponentially with dimensions (Kandasamy et al., 2015).

Various methods have been proposed to address the curses of dimensionality in BO. The vast majority of the prior work assumes special structures in the objective function, such as additive structure (Kandasamy et al., 2015; Han et al., 2021) or intrinsic dimension (Wang et al., 2016; Letham et al., 2020). However, these assumptions are often too restrictive for widespread application. Other works directly improve the high-dimensional BO without additional assumptions, including TuRBO (Eriksson et al., 2019), GIBO (Müller et al., 2021), and MPD (Nguyen et al., 2022).

This paper focuses on trust-region Bayesian Optimization (TuRBO). TuRBO is attractive because it uses local GPs for heterogeneous modeling of the objective function and performs BO locally in several trust regions to avoid over-exploration. However, using local GPs reduces sampling efficiency compared to a global GP. To overcome this limitation, we propose a new trust-region BO method (TuRBO-D) that incorporates the derivatives of GPs. It constructs several local quadratic models using gradients and Hessians from a global GP, enabling heterogeneous modeling of the objective function while maintaining the same sample efficiency of a global GP. To optimize globally, it maintains multiple trust regions simultaneously. Our method consists of three main stages: building

several local quadratic models using derivatives from a global GP, selecting new sample points by solving the bound-constrained quadratic program in each trust region, and updating the trust region radii based on new evaluations. In addition, we provide theoretical proof that our method converges to stationary points with high probability. In summary, our main contributions are:

- Proposing a new trust-region BO method that incorporates GP derivatives to enhance sampling efficiency while retaining heterogeneous modeling.
- Providing a convergence analysis guaranteeing the convergence of our proposed method.
- Empirically validating our method on synthetic and real-world applications, demonstrating improved efficacy over TuRBO and outperforming various high-dimensional BO methods.

2 RELATED WORK

In the realm of high-dimensional BO, there are generally three kinds of methods. The first kind of method assumes the existence of a lower-dimensional structure within objective functions, typically employing a three-stage process: producing a low-dimensional embedding, performing standard BO in this low-dimensional space, and projecting found optimal points back to the original space. In REMBO (Wang et al., 2016), the low-dimensional embedding is achieved by using a random projection matrix. But REMBO often produces points that fall outside the box bounds of the original space, necessitating their projection onto the facet of the box and resulting in a harmful distortion. Subsequently, several techniques are proposed to fix this problem (Letham et al., 2020; Binois et al., 2020). In addition, the random low-dimensional embedding can be also achieved by randomized hashing functions (Nayebi et al., 2019; Papenmeier et al., 2022). The key advantage of the hashing functions lies in their ability to effortlessly map candidate points back to the original space, thus circumventing the need for clipping to box-bound facets. Some works achieve linear embeddings based on learning. For example, SIR-BO employs Sliced Inverse Regression to derive the linear embeddings, while SI-BO (Djolonga et al., 2013) learns the linear embeddings via low-rank matrix recovery. Garnett et al. (2014) learn the linear embeddings by maximizing the marginal likelihood of GPs. Besides, nonlinear embedding techniques have also been explored, particularly those based on Variational Autoencoders (Gómez-Bombarelli et al., 2018; Lu et al., 2018). However, these approaches typically require a substantially larger sample size. In addition to embedding techniques, some research has focused on variable selection methods (Kirschner et al., 2019; Li et al., 2017; Shen & Kingsford, 2023; Song et al., 2022).

The second kind of method assumes the existence of an additive structure for the objective function. The additive objective function can be modeled by additive GPs (Kandasamy et al., 2015), allowing for more efficient maximization of the acquisition function. However, the true additive structure still remains challenging to learn. Several works propose to learn the underlying additive structure from training data. For example, Wang et al. (2017) proposed a method that employs the Dirichlet process to assign input variables into distinct groups. Rolland et al. (2018) employ a dependency graph to model the interactions between input variables, allowing for the assignment of input variables into overlapping groups. Han et al. (2021) proposed a refinement that restricts the dependency graph to a tree structure, reducing the computational complexity of maximizing acquisition functions. In contrast to data-driven decomposition methods, RDUCB (Ziomek & Bou-Ammar, 2023) learns a random tree-based decomposition to mitigate the potential mismatch between the objective function and additive GPs.

The third kind of method focuses on direct enhancements to the BO process in high-dimensional spaces, without relying on any other assumption. For example, TuRBO (Eriksson et al., 2019), GIBO (Müller et al., 2021) and MPD (Nguyen et al., 2022) adopt local strategies for BO to avoid over-exploration in high-dimensional spaces. Another set of approaches focuses on partitioning the search space and identifying a promising region to perform BO more efficiently (Wang et al., 2014; Kawaguchi et al., 2015; Wang et al., 2020). Researchers have also proposed better initialization methods for optimizing high-dimensional acquisition functions efficiently (Rana et al., 2017; Zhao et al., 2024).

GIBO and MPD are similar to ours, which also utilize gradients of GPs. In contrast to their work, our work incorporates both gradient and Hessian information from GPs and provides a convergence analysis.

108 **3 BACKGROUND**

109
110 **3.1 BAYESIAN OPTIMIZATION**
111

112 Bayesian optimization considers an optimization problem $\min_{\mathbf{x} \in \mathcal{X}} f(\mathbf{x})$ where f is a black-box
113 and derivative-free function over a hyper-rectangular feasible set \mathcal{X} . As a sequential model-based
114 approach, BO comprises two main components: a surrogate model and an acquisition function. The
115 surrogate model approximates the objective function, while the acquisition function, based on this
116 model, determines the next sampling point. Gaussian Process regression is typically employed as the
117 surrogate model (Rasmussen & Williams, 2006), $f \sim \mathcal{GP}(m(\cdot), k(\cdot, \cdot))$ with a mean function $m(\cdot)$
118 and a kernel $k(\cdot, \cdot)$. More specifically, GP assumes that evaluations of any finite number sampling
119 point $\mathbf{x}_{1:n}$ follow a joint Gaussian distribution, $\mathbf{f} \sim \mathcal{N}(\mathbf{m}(\mathbf{x}_{1:n}), \mathbf{K}(\mathbf{x}_{1:n}, \mathbf{x}_{1:n}))$. Given training
120 data $\mathcal{D}_n = \{\mathbf{x}_{1:n}, \mathbf{y}_{1:n}\}$ and a new point \mathbf{x}_* , the joint distribution is given by
121

$$\begin{bmatrix} \mathbf{y}_{1:n} \\ f(\mathbf{x}_*) \end{bmatrix} \sim \mathcal{N} \left(\begin{bmatrix} \mathbf{m}(\mathbf{x}_{1:n}) \\ m(\mathbf{x}_*) \end{bmatrix}, \begin{bmatrix} \mathbf{K}(\mathbf{x}_{1:n}, \mathbf{x}_{1:n}) + \sigma_n^2 \mathbf{I} & \mathbf{k}(\mathbf{x}_{1:n}, \mathbf{x}_*) \\ \mathbf{k}(\mathbf{x}_*, \mathbf{x}_{1:n}) & k(\mathbf{x}_*, \mathbf{x}_*) \end{bmatrix} \right)$$

122 where σ_n^2 is the variance of Gaussian noise added to the observations. It follows from the
123 Sherman-Morrison-Woodbury formula that the posterior normal distribution for $f(\mathbf{x}_*)$ is given by
124 $f(\mathbf{x}_*) | \mathcal{D}_n, \mathbf{x}_* \sim \mathcal{N}(\mu_n(\mathbf{x}_*), \sigma_n^2(\mathbf{x}_*))$ where
125

$$\begin{aligned} \mu_n(\mathbf{x}_*) &= m(\mathbf{x}_*) + \mathbf{k}(\mathbf{x}_*, \mathbf{x}_{1:n})(\mathbf{K}(\mathbf{x}_{1:n}, \mathbf{x}_{1:n}) + \sigma_n^2 \mathbf{I})^{-1}(\mathbf{y}_{1:n} - \mathbf{m}(\mathbf{x}_{1:n})) \\ \sigma_n^2(\mathbf{x}_*) &= k(\mathbf{x}_*, \mathbf{x}_*) - \mathbf{k}(\mathbf{x}_*, \mathbf{x}_{1:n})(\mathbf{K}(\mathbf{x}_{1:n}, \mathbf{x}_{1:n}) + \sigma_n^2 \mathbf{I})^{-1} \mathbf{k}(\mathbf{x}_{1:n}, \mathbf{x}_*) \end{aligned}$$

126 Based on this posterior, an acquisition function $\alpha(\cdot)$ is constructed to quantify the utility of sampling
127 points. Common choices include Expected Improvement (Jones et al., 1998) and Entropy Search
128 (Hennig & Schuler, 2012). The next sample point is determined by maximizing the acquisition
129 function, $\mathbf{x}_{n+1} = \arg \max_{\mathbf{x} \in \mathcal{X}} \alpha(\mathbf{x})$. After evaluating the objective function at \mathbf{x}_{n+1} , the process
130 advances to the next iteration.
131

132 **3.2 UNIFORM ERROR BOUNDS OF THE GP**
133

134 Under the mild assumption of Lipschitz continuity for both the objective function and the kernel
135 function, a directly computable probabilistic uniform error bound can be established.
136

137 **Assumption 1.** *The unknown objective function f is a sample from a Gaussian process
138 $\mathcal{GP}(0, k(\mathbf{x}, \mathbf{x}'))$ and observations are perturbed by Gaussian noise, $y = f(\mathbf{x}) + \epsilon$, where $\epsilon \sim
139 \mathcal{N}(0, \sigma^2)$. The unknown function f is continuous with the Lipschitz constant L_f and the kernel k is
140 Lipschitz continuous with the Lipschitz constant defined as*
141

$$L_k := \max_{\mathbf{x}, \mathbf{x}' \in \mathcal{X}} \left\| \left(\frac{\partial k(\mathbf{x}, \mathbf{x}')}{\partial x_1}, \dots, \frac{\partial k(\mathbf{x}, \mathbf{x}')}{\partial x_D} \right)^\top \right\|_2.$$

142 **Theorem 1** (Theorem 3.1 in (Lederer et al., 2019)). *Given an unknown function f satisfying Assumption 1, the posterior mean function μ_t from the GP fitted on the training data \mathcal{D}_t is continuous
143 with the Lipschitz constant L_{μ_t} , and the standard deviation σ_t admits a modulus of continuity ω_{σ_t}
144 on \mathcal{X} , where*
145

$$L_{\mu_t} \leq L_k \sqrt{t} \|(\mathbf{K} + \sigma_t^2 \mathbf{I})^{-1} \mathbf{y}\|_2$$

$$\omega_{\sigma_t}(\tau) \leq \sqrt{2\tau L_k \left(1 + t \|(\mathbf{K} + \sigma_t^2 \mathbf{I})^{-1}\|_2 \max_{\mathbf{x}, \mathbf{x}' \in \mathcal{X}} k(\mathbf{x}, \mathbf{x}') \right)}.$$

146 Moreover, given $\delta \in (0, 1)$, $\tau > 0$, one has that
147

$$\mathbb{P}(|f(\mathbf{x}) - \mu_t(\mathbf{x})| \leq \sqrt{\beta(\tau)} \sigma_t(\mathbf{x}) + \gamma(\tau), \forall \mathbf{x} \in \mathcal{X}) \geq 1 - \delta, \quad (1)$$

148 where
149

$$\beta(\tau) = 2 \log \left(\frac{M(\tau, \mathcal{X})}{\delta} \right), \quad \gamma(\tau) = (L_{\mu_t} + L_f)\tau + \sqrt{\beta(\tau)} \omega_{\sigma_t}(\tau),$$

150 and $M(\tau, \mathcal{X})$ is the covering number that is the minimum number of spherical balls with radius τ
151 required to completely cover \mathcal{X} .
152

162 **4 METHOD**
 163

164 In this section, we propose a novel trust-region BO method for optimizing high-dimensional black-
 165 box functions. To address the reduced sampling efficiency of local GPs in TuRBO, we construct
 166 several local quadratic models using gradients and Hessians from a global GP. This approach allows
 167 for heterogeneous modeling of the objective function while maintaining the same sample efficiency
 168 of a global GP. To achieve global optimization, we select new sample points by solving the bound-
 169 constrained quadratic programs in multiple regions.
 170

171 **Local modeling.** At iteration k , with \mathbf{x}_k as the best solution found so far, the local quadratic model
 172 is defined as,

$$m_k(\mathbf{x}_k + \mathbf{s}) = f(\mathbf{x}_k) + \mathbf{g}_k^\top \mathbf{s} + \frac{1}{2} \mathbf{s}^\top \mathbf{B}_k \mathbf{s}, \quad (2)$$

175 where \mathbf{g}_k and \mathbf{B}_k approximate the gradient and Hessian of the objective function, respectively. Since
 176 the derivatives of the objective function f are unknown, we set

$$\mathbf{g}_k = \nabla \mu_k(\mathbf{x}_k), \quad \mathbf{B}_k = \nabla^2 \mu_k(\mathbf{x}_k) + \lambda \nabla^2 \sigma_k(\mathbf{x}_k),$$

179 where λ is a hyperparameter, $\mu_k(\cdot)$ and $\sigma_k(\cdot)$ are the posterior mean and standard deviation of the
 180 GP model.
 181

182 **Trust regions.** To ensure the quadratic model m_k accurately approximates f , $\mathbf{x}_k + \mathbf{s}$ needs to be
 183 restricted to a trust region \mathcal{B}_k defined as
 184

$$\mathcal{B}_k := \{\mathbf{x} \in \mathbb{R}^D \mid \|\mathbf{x} - \mathbf{x}_k\| \leq \Delta_k\},$$

186 where Δ_k is the trust-region radius, adjusted iteratively. It should be decreased when the optimizer
 187 appears stuck and increased when the optimizer finds better solutions. When the radius falls below
 188 a predetermined minimum threshold Δ_{\min} , it signals that the current region has been thoroughly
 189 explored. At this point, the algorithm restarts in another region to promote global exploration.
 190 In this paper, we adopt the same radius update strategy as TuRBO, which has proven effective in
 191 balancing local exploitation and global exploration.
 192

193 **Trust regions in the ∞ -norm.** In BO, the search space is typically a rectangular box. Without
 194 loss of generality, we assume that the box is $[0, 1]^D$. Given this constraint, the trust region is defined
 195 as

$$\mathcal{B}_k := \{\mathbf{x} \in \mathbb{R}^D \mid \|\mathbf{x} - \mathbf{x}_k\| \leq \Delta_k, \mathbf{0} \leq \mathbf{x} \leq \mathbf{1}\}.$$

198 When the trust region is in the Euclidean norm, \mathcal{B}_k consists of the intersection of a sphere and a
 199 rectangular (Jorge & Stephen, 2006), leading to more complex quadratic models. To simplify this,
 200 we adopt the ∞ -norm for the trust region, which transforms \mathcal{B}_k into a simple rectangular,

$$\mathcal{B}_k := \{\mathbf{x} \in \mathbb{R}^D \mid -\Delta_k \mathbf{1} \leq \mathbf{x} - \mathbf{x}_k \leq \Delta_k \mathbf{1}, \mathbf{0} \leq \mathbf{x} \leq \mathbf{1}\}.$$

203 Then candidate is selected by solving the bound-constrained quadratic program,

$$\underset{\mathbf{s}}{\text{minimize}} \quad m_k(\mathbf{x}_k + \mathbf{s}), \quad \text{subject to } \mathbf{x}_k + \mathbf{s} \in \mathcal{B}_k. \quad (3)$$

206 The above problem can be solved by gradient projection methods. However, the Hessian of the GP
 207 is often nearly singular, which can lead to issues when using conjugate gradient iterations. Such
 208 methods may require numerous iterations and yield only small reductions in each step. Instead, we
 209 employ a gradient projection method using quasi-Newton iterations, specifically L-BFGS-B (Byrd
 210 et al., 1995). This approach approximates the singular Hessian with a positive definite matrix, im-
 211 proving the efficiency and robustness of the optimization process.
 212

213 **Derivatives vanish in the high-dimensional space.** In general, our approach is effective for
 214 medium-dimensional problems (typically $D < 100$). However, as the dimensionality increases be-
 215 yond this range, the derivatives of GPs tend to vanish, posing a significant challenge to our method.
 To mitigate this issue and ensure the derivatives remain informative, we choose d variables out of D

variables randomly as the working set \mathcal{W}_k at each iteration. Then, a global GP is constructed on the working set and the bound-constrained quadratic program is denoted as

$$\begin{aligned} \underset{\mathbf{s}}{\text{minimize}} \quad & m_k(\mathbf{x}_k + \mathbf{s}) = f(\mathbf{x}_k) + \mathbf{g}_k^\top \mathbf{s} + \frac{1}{2} \mathbf{s}^\top \mathbf{B}_k \mathbf{s}, \\ \text{subject to} \quad & \mathbf{s}_i = 0, \forall i \notin \mathcal{W}_k \\ & \mathbf{x}_k + \mathbf{s} \in \mathcal{B}_k. \end{aligned} \quad (4)$$

So far, we have detailed a single local BO strategy using a trust region. To achieve global optimization in this framework, we maintain m trust regions simultaneously, selecting a candidate within each trust region to form a batch of m candidates. We denote our method as TuRBO-D, as presented in Algorithm 1.

Algorithm 1: TuRBO-D

Input: n, T, M

Output: The sample points and their evaluations \mathcal{D}_T

```

1  $\mathcal{D}_0 = \{\mathbf{x}_{1:n}, \mathbf{y}_{1:n}\} \leftarrow$  Randomly sample  $n$  points from the feasible set  $\mathcal{X}$  and then evaluate
2 these points;
3 Initializations. Choose an initial radius for each trust region,  $\{\Delta_0^{(\ell)}\}_{\ell=1}^M$ , and determine an
4 initial point for each trust region,  $\{\mathbf{x}_0^{(\ell)}\}_{\ell=1}^M \subset \mathcal{D}_0$ ;
5 for  $k \leftarrow 1$  to  $T$  do
6   Build a global GP based on the training data  $\mathcal{D}_k$ ;
7   for  $\ell \leftarrow 1$  to  $M$  do
8     Build a local quadratic model  $m_k^{(\ell)}(\mathbf{x}_k^{(\ell)} + \mathbf{s})$  in the  $\ell$ -th trust region;
9     Select a candidate by minimizing the model within the  $\ell$ -th trust region according to
10    Eq.3;
11    Evaluate the candidate,  $y_{k+1}^{(\ell)} \leftarrow f(\mathbf{x}_{k+1}^{(\ell)})$ ;
12    Update the trust-region radius  $\Delta_k^{(\ell)}$  based on new evaluations;
13   Update the training data,  $\mathcal{D}_{k+1} \leftarrow \mathcal{D}_k \cup \{\mathbf{x}_{k+1}^{(\ell)}, y_{k+1}^{(\ell)}\}_{\ell=1}^M$ ;
14 return  $\mathcal{D}_T$ 

```

5 A CONVERGENCE ANALYSIS

Our method shares several key features with trust-region derivative-free optimization methods, including the use of quadratic models to approximate the objective function and adaptive trust region updates. However, a crucial distinction lies in the nature of the error between the quadratic model and the objective function. This error is probabilistic in our approach, while it is typically deterministic in derivative-free optimization methods using interpolation techniques. This probabilistic aspect necessitates a verification of the coherence between the derivatives of GPs and those of the objective function. This fundamental difference precludes the direct application of standard convergence theory for derivative-free methods to our method. Consequently, we must reconsider the convergence analysis in detail.

To maintain analytical simplicity, we adopt the same assumptions as (Conn et al., 1997) and follow their trust region update strategy, as outlined in Algorithm 2.

Assumption 2. *The objective function $f : \mathbb{R}^D \rightarrow \mathbb{R}$ is twice continuously differentiable whose gradient $\nabla f(\mathbf{x})$ and Hessian $\nabla^2 f(\mathbf{x})$ is uniformly bounded in the norm. In other words, there are constants $\kappa_{fg} > 0$ and $\kappa_{fh} > 0$ such that*

$$\|\nabla f(\mathbf{x})\|_2 \leq \kappa_{fg}, \quad \|\nabla^2 f(\mathbf{x})\|_2 \leq \kappa_{fh}$$

for all $\mathbf{x} \in \mathbb{R}^D$.

Assumption 3. *The objective function is bounded below on \mathbb{R}^D .*

Assumption 4. *The approximate Hessians \mathbf{B}_k are uniformly bounded in the norm. In other words, there is a constant $\kappa_{mh} > 0$ such that $\|\mathbf{B}_k\|_2 \leq \kappa_{mh}$, $\forall \mathbf{x} \in \mathcal{B}_k$.*

270 **Algorithm 2:** The trust-region update strategy in derivative-free optimization
271 **Input:** \mathbf{s}_k , Δ_k , $0 < \eta_0 \leq \eta_1 < 1$, $0 < \beta_1 < 1 < \beta_2$, $\mu \geq 1$
272 **Output:** Δ_{k+1}

273 1 Compute the ratio
274
$$\rho_k := \frac{f(\mathbf{x}_k) - f(\mathbf{x}_k + \mathbf{s}_k)}{m_k(\mathbf{x}_k) - m_k(\mathbf{x}_k + \mathbf{s}_k)}.$$

275 2 **if** $\rho_k \geq \eta_1$ **then**
276 2
$$\Delta_{k+1} \leftarrow \min\{\beta_2 \Delta_k, \mu \|\mathbf{g}_k\|_2\}.$$

277 3 **else if** $\rho_k < \eta_0$ **then**
278 3
$$\Delta_{k+1} \leftarrow \beta_1 \Delta_k.$$

279 4 **else**
280 5
$$\Delta_{k+1} \leftarrow \Delta_k;$$

281 6 **return** Δ_{k+1}

287
288
289 **Lemma 1** (Lemma 6 in (Conn et al., 1997)). At every iteration k , one has that

290
291
$$m_k(\mathbf{x}_k) - m_k(\mathbf{x}_k + \mathbf{s}_k) \geq \kappa_{mdc} \|\mathbf{g}_k\| \min\left(\Delta_k, \frac{\|\mathbf{g}_k\|}{\kappa_h}\right),$$

292

293 for some constant $\kappa_{mdc} \in (0, 1)$ independent of k , where $\kappa_h = \max\{\kappa_{fg}, \kappa_{fh}, \kappa_{mh}\}$.

294 **Theorem 2.** Assume that Assumption 1, 2, and 4 hold. Then given $\delta \in (0, 1)$ there is κ_{em} such that

295
296
$$\mathbb{P}(|f(\mathbf{x}) - m_k(\mathbf{x})| \leq \kappa_{em} \max\{\Delta_k, \Delta_k^2\}, \forall \mathbf{x} \in \mathcal{B}_k \forall k) \geq 1 - \delta.$$

297

298 *Proof.* It follows from Taylor's theorem that

299
300
$$f(\mathbf{x}_k + \mathbf{s}) = f(\mathbf{x}_k) + \nabla f(\mathbf{x}_k)^\top \mathbf{s} + \int_0^1 [\nabla f(\mathbf{x}_k + t\mathbf{s}) - \nabla f(\mathbf{x}_k)]^\top \mathbf{s} dt,$$

301

302 for some $t \in (0, 1)$. Then

303
304
$$\begin{aligned} & |m_k(\mathbf{x}_k + \mathbf{s}) - f(\mathbf{x}_k + \mathbf{s})| \\ &= \left| [\nabla \mu_k(\mathbf{x}_k) - \nabla f(\mathbf{x}_k)]^\top \mathbf{s} + \frac{1}{2} \mathbf{s}^\top \nabla^2 \mu_k(\mathbf{x}_k) \mathbf{s} - \int_0^1 [\nabla f(\mathbf{x}_k + t\mathbf{s}) - \nabla f(\mathbf{x}_k)]^\top \mathbf{s} dt \right| \\ &\leq \|\nabla \mu_k(\mathbf{x}_k) - \nabla f(\mathbf{x}_k)\|_2 \|\mathbf{s}\|_2 + (\kappa_{mh}/2) \|\mathbf{s}\|_2^2 + \kappa_{fh} \|\mathbf{s}\|_2^2 \end{aligned} \tag{5}$$

309 It follows from Eq. 1 that

310
311
$$\mathbb{P}\left(\|\nabla \mu_k(\mathbf{x}_k) - \nabla f(\mathbf{x}_k)\|_2 \leq \sqrt{\beta(\tau)} \|\nabla \sigma_k(\mathbf{x}_k)\|_2, \forall k\right) \geq 1 - \delta.$$

312 In fact, assume without loss of generality that $f(\mathbf{x}_k) - \mu_t(\mathbf{x}_k) \leq \sqrt{\beta(\tau)} \sigma_t(\mathbf{x}_k) + \gamma(\tau)$, then
313 following the continuity of $f(\mathbf{x})$, $\mu_t(\mathbf{x})$ and $\sigma_t(\mathbf{x})$, there is $\varepsilon \in (0, 1)$ such that $\forall i \in \{1, \dots, D\}$

314
315
$$f(\mathbf{x}_k + \varepsilon \mathbf{e}_i) - \mu_t(\mathbf{x}_k + \varepsilon \mathbf{e}_i) \leq \sqrt{\beta(\tau)} \sigma_t(\mathbf{x}_k + \varepsilon \mathbf{e}_i) + \gamma(\tau).$$

316 Hence, combining the above two inequalities, one has that

317
318
$$\frac{f(\mathbf{x}_k + \varepsilon \mathbf{e}_i) - f(\mathbf{x}_k)}{\varepsilon} - \frac{\mu_t(\mathbf{x}_k + \varepsilon \mathbf{e}_i) - \mu_t(\mathbf{x}_k)}{\varepsilon} \leq \sqrt{\beta(\tau)} \frac{\sigma_t(\mathbf{x}_k + \varepsilon \mathbf{e}_i) - \sigma_t(\mathbf{x}_k)}{\varepsilon}.$$

319 Letting $\varepsilon \rightarrow 0$, one has that

320
321
$$\frac{\partial f(\mathbf{x}_k)}{\partial x_i} - \frac{\partial \mu_t(\mathbf{x}_k)}{\partial x_i} \leq \sqrt{\beta(\tau)} \frac{\partial \sigma_t(\mathbf{x}_k)}{\partial x_i}.$$

324 Similarly, if $\mu_t(\mathbf{x}_k) - f(\mathbf{x}_k) \leq \sqrt{\beta(\tau)}\sigma_t(\mathbf{x}_k) + \gamma(\tau)$, then
 325

$$326 \frac{\partial \mu_t(\mathbf{x}_k)}{\partial x_i} - \frac{\partial f(\mathbf{x}_k)}{\partial x_i} \leq \sqrt{\beta(\tau)} \frac{\partial \sigma_t(\mathbf{x}_k)}{\partial x_i}, \forall i \in \{1 \dots D\}. \\ 327$$

328 Since then, it has been proved the event $|f(\mathbf{x}_k) - \mu_t(\mathbf{x}_k)| \leq \sqrt{\beta(\tau)}\sigma_t(\mathbf{x}_k) + \gamma(\tau)$ implies that
 329 $\|\nabla \mu_k(\mathbf{x}_k) - \nabla f(\mathbf{x}_k)\|_2 \leq \sqrt{\beta(\tau)}\|\nabla \sigma_k(\mathbf{x}_k)\|_2$.
 330

331 Since σ_k admits a modulus of continuity according to Theorem 1, there is κ_{eg} such that
 332 $\|\nabla \sigma_k(\mathbf{x}_k)\|_2 \leq \kappa_{eg}\Delta_k$. Then

$$333 \mathbb{P} \left(\|\nabla \mu_k(\mathbf{x}_k) - \nabla f(\mathbf{x}_k)\|_2 \leq \kappa_{eg}\sqrt{\beta(\tau)}\Delta_k, \forall k \right) \geq 1 - \delta. \quad (6) \\ 334$$

335 Combining Eq. 5 and 6, one has that
 336

$$337 \mathbb{P} \left[|m_k(\mathbf{x}_k + \mathbf{s}) - f(\mathbf{x}_k + \mathbf{s})| \leq (\kappa_{eg}\sqrt{\beta(\tau)} + \kappa_{mh}/2 + \kappa_{fh}) \max\{\Delta_k, \Delta_k^2\}, \forall k \right] \geq 1 - \delta \\ 338$$

339 Hence, $\kappa_{em} = \kappa_{eg}\sqrt{\beta(\tau)} + \kappa_{mh}/2 + \kappa_{fh}$. \square
 340

341 **Lemma 2.** Assume that Assumption 1-4 hold. In addition, assume that there is a constant $\kappa_g > 0$
 342 such that $\|g_k\| \geq \kappa_g$ for all k . Then given $\delta \in (0, 1)$ there is a constant κ_d such that
 343

$$\mathbb{P}(\Delta_k > \kappa_d, \forall k) \geq 1 - \delta.$$

344 *Proof.* It follows from Lemma 7 in (Conn et al., 1997) that if $|f(\mathbf{x}) - m_k(\mathbf{x})| \leq \kappa_{em} \max\{\Delta_k, \Delta_k^2\}$,
 345 then $\forall k$, $\Delta_k > \kappa_d$, where
 346

$$347 \kappa_d = \beta_1 \min \left(1, \frac{\kappa_{mdc}\kappa_g(1 - \eta_1)}{\max(\kappa_h, \kappa_{em})} \right).$$

349 And since it follows from Theorem 2 that
 350

$$351 \mathbb{P}(|f(\mathbf{x}) - m_k(\mathbf{x})| \leq \kappa_{em} \max\{\Delta_k, \Delta_k^2\}, \forall \mathbf{x} \in \mathcal{B}_k \forall k) \geq 1 - \delta.$$

352 and hence, we obtain
 353

$$\mathbb{P}(\Delta_k > \kappa_d, \forall k) \geq 1 - \delta.$$

355 \square
 356

357 This property ensures that the radius cannot become too small with a high probability as long as the
 358 gradient of the GP does not vanish.
 359

360 **Theorem 3.** Assume that Assumption 1-4 hold. Then it holds that
 361

$$\liminf_{k \rightarrow \infty} \|g_k\|_2 = 0$$

363 *Proof.* We proceed by contradiction. Suppose there is $\kappa_g > 0$ such that $\|g_k\| \geq \kappa_g$ for all k . It
 364 follows from Theorem 9 in (Conn et al., 1997) that if $\Delta_k > \kappa_d$ for all k , then
 365

$$366 f(\mathbf{x}_0) - f(\mathbf{x}_{k+1}) \geq \frac{1}{2} \sigma_k \kappa_g \eta_0 \min \left(\frac{\kappa_g}{\kappa_h}, \kappa_d \right)$$

368 where σ_k is the number of successful iterations up to iteration k . In our case, it follows from Lemma
 369 2 that
 370

$$\mathbb{P}(\Delta_k > \kappa_d, \forall k) \geq 1 - \delta.$$

371 This implies that
 372

$$373 \mathbb{P} \left(f(\mathbf{x}_0) - f(\mathbf{x}_{k+1}) \geq \frac{1}{2} \sigma_k \kappa_g \eta_0 \min \left(\frac{\kappa_g}{\kappa_h}, \kappa_d \right) \right) \geq 1 - \delta.$$

375 And since $\lim_{k \rightarrow \infty} \sigma_k = +\infty$, one has that $\forall M \in \mathbb{R} \exists k$,

$$376 \mathbb{P}(f(\mathbf{x}_0) - f(\mathbf{x}_{k+1}) > M) \geq 1 - \delta,$$

377 which contradicts the fact that f is bounded. \square

378 **Lemma 3.** Assume that Assumption 1-4 hold. If there is a subsequence $\{k_i\}$ such that
 379 $\lim_{i \rightarrow \infty} \|\mathbf{g}_{k_i}\| = 0$, then given $\delta \in (0, 1)$ it holds that $\forall \epsilon \in (0, 1) \exists N$,

$$381 \quad \mathbb{P}(\|\nabla f(\mathbf{x}_{k_i})\|_2 < \epsilon, \forall i > N) \geq 1 - \delta.$$

383 *Proof.* It follows from Eq. 6 that

$$384 \quad \mathbb{P}\left(\|\nabla f(\mathbf{x}_{k_i}) - \mathbf{g}_{k_i}\|_2 \leq \kappa_{eg} \sqrt{\beta(\tau)} \Delta_{k_i}, \forall i\right) \geq 1 - \delta.$$

386 And since $\Delta_{k_i} \leq \mu \|\mathbf{g}_{k_i}\|_2$ (according to Algo. 2), one has that

$$388 \quad \mathbb{P}\left(\|\nabla f(\mathbf{x}_{k_i}) - \mathbf{g}_{k_i}\|_2 \leq \kappa_{eg} \sqrt{\beta(\tau)} \mu \|\mathbf{g}_{k_i}\|_2, \forall i\right) \geq 1 - \delta.$$

390 And since $\|\nabla f(\mathbf{x}_{k_i})\|_2 \leq \|\mathbf{g}_{k_i}\|_2 + \|\nabla f(\mathbf{x}_{k_i}) - \mathbf{g}_{k_i}\|_2$, one has that

$$392 \quad \mathbb{P}\left(\|\nabla f(\mathbf{x}_{k_i})\|_2 \leq (1 + \kappa_{eg} \sqrt{\beta(\tau)} \mu) \|\mathbf{g}_{k_i}\|_2, \forall i\right) \geq 1 - \delta.$$

394 Combining the limit $\lim_{i \rightarrow \infty} \|\mathbf{g}_{k_i}\|_2 = 0$ and the above equation, one has that $\forall \epsilon \in (0, 1) \exists N$,

$$395 \quad \mathbb{P}(\|\nabla f(\mathbf{x}_{k_i})\|_2 < \epsilon, \forall i > N) \geq 1 - \delta.$$

□

399 **Theorem 4.** Assume that Assumption 1-4 hold. Then given $\delta \in (0, 1)$, there is a sequence of
 400 iterations $\{\mathbf{x}_k\}$ such that $\forall \epsilon \in (0, 1) \exists N$,

$$401 \quad \mathbb{P}\left(\inf_{k > N} \|\nabla f(\mathbf{x}_k)\| = 0\right) \geq 1 - \delta.$$

404 *Proof.* The result immediately follows from Theorem 3 and Lemma 3. □

406 The theorem ensures that our approach will converge to stationary points with a high probability.

409 6 EXPERIMENTAL RESULTS

411 In this section, we evaluate our method (TuRBO-D) on a wide range of benchmarks: 50-dimensional
 412 synthetic functions, 100-dimensional synthetic functions, a 300-dimensional Lasso tuning problem,
 413 a 180-dimensional Lasso tuning problem, and a 124-dimensional vehicle design problem.

414 We compare our method (TuRBO-D) to a broad selection of existing methods: linear embedding
 415 methods (ALEBO (Letham et al., 2020), SIR-BO), nonlinear embedding methods (KSIR-BO
 416 (Zhang et al., 2019)), BO using additive models (Add-GP-UCB (Kandasamy et al., 2015)), local-
 417 search methods (TuRBO, GIBO), and quasirandom search (Sobol). For BO using embedding, we
 418 take $d = 10$ for these experiments. For Add-GP-UCB, we take $d = 4$ for each group. TuRBO-D and
 419 TuRBO maintain 5 trust regions simultaneously. In 100-dimensional synthetic functions, Lasso and
 420 MOPTA08, we choose 50 variables randomly as the working set at each iteration for TuRBO-D to
 421 ensure derivatives of GPs remain informative. We test all methods using 50 initial points and batch
 422 size of $q = 5$.

423 6.1 SYNTHETIC EXPERIMENTS

425 First, we consider the 50-dimensional Ackley function in the domain $[-5, 10]^{50}$, and the 50-
 426 dimensional Griewank function in the domain $[-300, 600]^{50}$. Both functions feature numerous
 427 local minima and a global minimum, making them suitable for testing global optimization methods.
 428 Fig. 1 shows that TuRBO-D enhances the efficacy of TuRBO and gets the best performance of all
 429 methods on the mid-dimensional synthetic functions. The initialization strategy of ALEBO favors
 430 sampling points away from the boundary, resulting in high-quality initial samples. However, the
 431 optimizer of ALEBO tends to stagnate when objective functions lack lower-dimensional structure.
 SIR-BO and KSIR-BO demonstrate poor performance in this problem, yielding results comparable

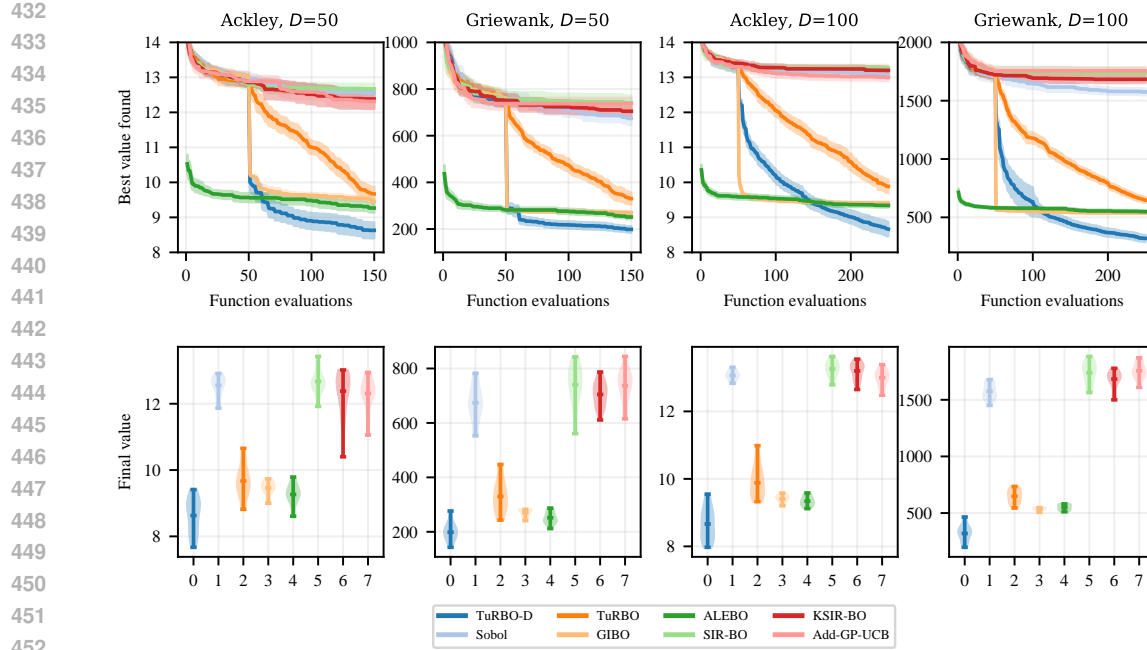


Figure 1: We compare TuRBO-D to baseline methods on 50-dimensional functions and 100-dimensional functions, showing (Top row) optimal values by each iteration averaged over 20 repeated runs, and (Bottom row) the distribution over the final optimal values over 20 repeated runs.

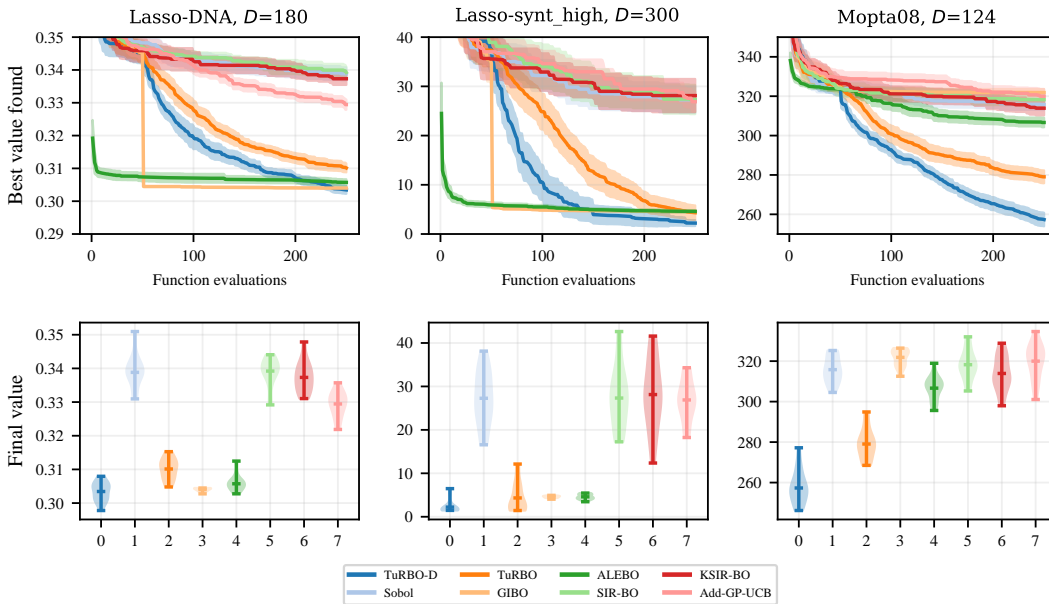


Figure 2: We compare TuRBO-D to baseline methods on the Lasso-DNA tuning ($D = 180$), Lasso-synt_high tuning ($D = 300$) and MOPTA vehicle design ($D = 124$), showing (Top row) optimal values by each iteration averaged over 20 repeated runs, and (Bottom row) the distribution over the final optimal values over 20 repeated runs.

to random search. Add-GP-UCB also underperforms on this problem because objective functions lack additive structure.

486 Second, we consider the 100-dimensional Ackley function in the domain $[-5, 10]^{100}$, and the 50-
 487 dimensional Griewank function in the domain $[-300, 600]^{100}$. Fig. 1 shows that TuRBO-D again
 488 enhances the efficacy of TuRBO and gets the best performance among all methods on the high-
 489 dimensional synthetic functions. GIBO always samples the midpoint of the domain after initial-
 490 ization. It suffers from the vanishing gradients of GPs in the high-dimensional spaces, causing
 491 it to become stuck at the midpoint. ALEBO once again encounters stagnation after initialization
 492 due to the absence of lower-dimensional structure in these functions. SIR-BO, KSIR-BO and Add-
 493 GP-UCB underperform on these high-dimensional functions without lower-dimensional structure or
 494 additive structure.

495

496

497 6.2 REAL-WORLD PROBLEMS

498

499 **Weighted Lasso Tuning.** We consider the problem of tuning the Lasso (Least Absolute Shrink-
 500 age and Selection Operator) regression models. LassoBench (Sehic et al., 2022) provides a set of
 501 benchmark problems for tuning penalty terms for Lasso models. In Lasso, each regression coeffi-
 502 cient corresponds to a penalty term, so the number of hyperparameters equals the number of features
 503 in the dataset. We focus on two Lasso tuning problems: a 180-dimensional DNA dataset with 43
 504 effective dimensions, and a 300-dimensional synthetic dataset with 15 effective dimensions.

505 Fig. 2 shows that TuRBO-D enhances the efficacy of TuRBO and achieves the best performance
 506 among all methods on the Lasso-synt_high problem. For the Lasso-DNA problem, TuRBO-D even-
 507 tually attains optimal values comparable to GIBO while outperforming other methods. GIBO, after
 508 initially sampling the midpoint, stagnates due to vanishing gradients of GPs in high-dimensional
 509 spaces. Its performance is primarily attributed to this initial midpoint sampling. ALEBO also be-
 510 comes stuck after initialization, despite the existence of lower-dimensional structure in these prob-
 511 lems. SIR-BO and KSIR-BO perform poorly, yielding results comparable to random search. Inter-
 512 estingly, Add-GP-UCB shows better performance than SIR-BO and KSIR-BO, despite LassoBench
 513 lacking the additive structure that Add-GP-UCB typically exploits.

514

515

516 **Vehicle Design.** We consider the vehicle design problem with a soft penalty as defined in (Eriksson
 517 & Jankowiak, 2021). The objective is to minimize the mass of a vehicle characterized by 124
 518 design variables describing materials, gauges, and vehicle shape. This results in a 124-dimensional
 519 optimization problem.

520

521

522

523

524

525

526

527

528

7 CONCLUSION

529

530 In this paper, we introduce TuRBO-D, a novel trust-region BO method that incorporates the deriva-
 531 tives of GPs for enhancing the sampling efficiency of TuRBO. This novel scheme is realized by (1)
 532 constructing several local quadratic models using gradients and Hessians from a global GP, enabling
 533 heterogeneous modeling of the objective function while maintaining the same sample efficiency of a
 534 global GP, and (2) selecting new sample points by solving the bound-constrained quadratic program
 535 in multiple trust regions. Comprehensive experimental evaluations demonstrate that TuRBO-D sig-
 536 nificantly enhances the efficacy of TuRBO and outperforms a wide range of high-dimensional BO
 537 methods on a set of synthetic functions and three real-world applications. Furthermore, we provide
 538 a convergence analysis for our method.

539

While we mitigate the problem of vanishing derivatives using working sets, we will focus on devel-
 oping better schemes to address this challenge in the future.

540 REFERENCES
541

- 542 Mickaël Binois, David Ginsbourger, and Olivier Roustant. On the choice of the low-
543 dimensional domain for global optimization via random embeddings. *J. Glob. Optim.*, 76(1):
544 69–90, 2020. doi: 10.1007/S10898-019-00839-1. URL <https://doi.org/10.1007/s10898-019-00839-1>.
- 545 Richard H. Byrd, Peihuang Lu, Jorge Nocedal, and Ciyou Zhu. A limited memory algorithm for
546 bound constrained optimization. *SIAM Journal on Scientific Computing*, 16(5):1190–1208, 1995.
547 doi: 10.1137/0916069. URL <https://doi.org/10.1137/0916069>.
- 548 Andrew R Conn, Katya Scheinberg, and Ph L Toint. On the convergence of derivative-free methods
549 for unconstrained optimization. *Approximation theory and optimization: tributes to MJD Powell*,
550 pp. 83–108, 1997.
- 551 Josip Djolonga, Andreas Krause, and Volkan Cevher. High-dimensional gaussian pro-
552 cess bandits. In Christopher J. C. Burges, Léon Bottou, Zoubin Ghahramani, and
553 Kilian Q. Weinberger (eds.), *Advances in Neural Information Processing Systems 26:
554 27th Annual Conference on Neural Information Processing Systems 2013. Proceedings
555 of a meeting held December 5-8, 2013, Lake Tahoe, Nevada, United States*, pp.
556 1025–1033, 2013. URL <https://proceedings.neurips.cc/paper/2013/hash/8d34201a5b85900908db6cae92723617-Abstract.html>.
- 557 David Eriksson and Martin Jankowiak. High-dimensional bayesian optimization with sparse axis-
558 aligned subspaces. In Cassio P. de Campos, Marloes H. Maathuis, and Erik Quaeghebeur
559 (eds.), *Proceedings of the Thirty-Seventh Conference on Uncertainty in Artificial Intelligence,
560 UAI 2021, Virtual Event, 27-30 July 2021*, volume 161 of *Proceedings of Machine Learning
561 Research*, pp. 493–503. AUAI Press, 2021. URL <https://proceedings.mlr.press/v161/eriksson21a.html>.
- 562 David Eriksson, Michael Pearce, Jacob R. Gardner, Ryan Turner, and Matthias Poloczek. Scalable
563 global optimization via local bayesian optimization. In Hanna M. Wallach, Hugo Larochelle,
564 Alina Beygelzimer, Florence d’Alché-Buc, Emily B. Fox, and Roman Garnett (eds.), *Advances
565 in Neural Information Processing Systems 32: Annual Conference on Neural Information Pro-
566 cessing Systems 2019, NeurIPS 2019, December 8-14, 2019, Vancouver, BC, Canada*, pp.
567 5497–5508, 2019. URL <https://proceedings.neurips.cc/paper/2019/hash/6c990b7aca7bc7058f5e98ea909e924b-Abstract.html>.
- 568 Roman Garnett, Michael A. Osborne, and Philipp Hennig. Active learning of lin-
569 ear embeddings for gaussian processes. In Nevin L. Zhang and Jin Tian (eds.),
570 *Proceedings of the Thirtieth Conference on Uncertainty in Artificial Intelligence, UAI
571 2014, Quebec City, Quebec, Canada, July 23-27, 2014*, pp. 230–239. AUAI Press,
572 2014. URL https://dslpitt.org/uai/displayArticleDetails.jsp?mmnu=1&smnu=2&article_id=2458&proceeding_id=30.
- 573 Rafael Gómez-Bombarelli, Jennifer N Wei, David Duvenaud, José Miguel Hernández-Lobato,
574 Benjamín Sánchez-Lengeling, Dennis Sheberla, Jorge Aguilera-Iparraguirre, Timothy D Hirzel,
575 Ryan P Adams, and Alán Aspuru-Guzik. Automatic chemical design using a data-driven contin-
576 uous representation of molecules. *ACS central science*, 4(2):268–276, 2018.
- 577 László Györfi, Michael Kohler, Adam Krzyzak, Harro Walk, et al. *A distribution-free theory of
578 nonparametric regression*, volume 1. Springer, 2002.
- 579 Eric Han, Ishank Arora, and Jonathan Scarlett. High-dimensional bayesian optimization via tree-
580 structured additive models. In *Thirty-Fifth AAAI Conference on Artificial Intelligence, AAAI
581 2021, Thirty-Third Conference on Innovative Applications of Artificial Intelligence, IAAI 2021,
582 The Eleventh Symposium on Educational Advances in Artificial Intelligence, EAAI 2021, Virtual
583 Event, February 2-9, 2021*, pp. 7630–7638. AAAI Press, 2021. doi: 10.1609/AAAI.V35I9.16933.
584 URL <https://doi.org/10.1609/aaai.v35i9.16933>.
- 585 Philipp Hennig and Christian J. Schuler. Entropy search for information-efficient global opti-
586 mization. *J. Mach. Learn. Res.*, 13:1809–1837, 2012. doi: 10.5555/2503308.2343701. URL
587 <https://dl.acm.org/doi/10.5555/2503308.2343701>.

- 594 Carl Hvarfner, Danny Stoll, Artur L. F. Souza, Marius Lindauer, Frank Hutter, and Luigi Nardi.
 595 \$\\pi\$bo: Augmenting acquisition functions with user beliefs for bayesian optimization. In
 596 *The Tenth International Conference on Learning Representations, ICLR 2022, Virtual Event,*
 597 April 25-29, 2022. OpenReview.net, 2022. URL <https://openreview.net/forum?id=MMAeCXIa89>.
- 598
- 599 Donald R. Jones, Matthias Schonlau, and William J. Welch. Efficient global optimization of expen-
 600 sive black-box functions. *J. Glob. Optim.*, 13(4):455–492, 1998. doi: 10.1023/A:1008306431147.
 601 URL <https://doi.org/10.1023/A:1008306431147>.
- 602
- 603 Nocedal Jorge and J Wright Stephen. *Numerical optimization*. Springer, 2006. ISBN
 604 9780387303031.
- 605
- 606 Kirthevasan Kandasamy, Jeff G. Schneider, and Barnabás Póczos. High dimensional bayesian opti-
 607 misation and bandits via additive models. In Francis R. Bach and David M. Blei (eds.), *Proceed-
 608 ings of the 32nd International Conference on Machine Learning, ICML 2015, Lille, France, 6-11
 609 July 2015*, volume 37 of *JMLR Workshop and Conference Proceedings*, pp. 295–304. JMLR.org,
 610 2015. URL <http://proceedings.mlr.press/v37/kandasamy15.html>.
- 611
- 612 Kenji Kawaguchi, Leslie Pack Kaelbling, and Tomás Lozano-Pérez. Bayesian optimization with ex-
 613 ponential convergence. In Corinna Cortes, Neil D. Lawrence, Daniel D. Lee, Masashi Sugiyama,
 614 and Roman Garnett (eds.), *Advances in Neural Information Processing Systems 28: Annual Con-
 615 ference on Neural Information Processing Systems 2015, December 7-12, 2015, Montreal, Que-
 616 bec, Canada*, pp. 2809–2817, 2015. URL <https://proceedings.neurips.cc/paper/2015/hash/0ebcc77dc72360d0eb8e9504c78d38bd-Abstract.html>.
- 617
- 618 Johannes Kirschner, Mojmir Mutny, Nicole Hiller, Rasmus Ischebeck, and Andreas Krause. Adap-
 619 tive and safe bayesian optimization in high dimensions via one-dimensional subspaces. In Ka-
 620 malika Chaudhuri and Ruslan Salakhutdinov (eds.), *Proceedings of the 36th International Con-
 621 ference on Machine Learning, ICML 2019, 9-15 June 2019, Long Beach, California, USA*, vol-
 622 ume 97 of *Proceedings of Machine Learning Research*, pp. 3429–3438. PMLR, 2019. URL
 623 <http://proceedings.mlr.press/v97/kirschner19a.html>.
- 624
- 625 Armin Lederer, Jonas Umlauft, and Sandra Hirche. Uniform error bounds for gaussian pro-
 626 cess regression with application to safe control. In Hanna M. Wallach, Hugo Larochelle,
 627 Alina Beygelzimer, Florence d’Alché-Buc, Emily B. Fox, and Roman Garnett (eds.), *Ad-
 628 vances in Neural Information Processing Systems 32: Annual Conference on Neural Infor-
 629 mation Processing Systems 2019, NeurIPS 2019, December 8-14, 2019, Vancouver, BC, Canada*,
 630 pp. 657–667, 2019. URL <https://proceedings.neurips.cc/paper/2019/hash/fc73f687e5bc5280214e0486b273a5f9-Abstract.html>.
- 631
- 632 Benjamin Letham, Roberto Calandra, Akshara Rai, and Eytan Bakshy. Re-examining
 633 linear embeddings for high-dimensional bayesian optimization. In Hugo Larochelle,
 634 Marc’Aurelio Ranzato, Raia Hadsell, Maria-Florina Balcan, and Hsuan-Tien Lin (eds.),
 635 *Advances in Neural Information Processing Systems 33: Annual Conference on Neu-
 636 ral Information Processing Systems 2020, NeurIPS 2020, December 6-12, 2020, vir-
 637 tual*, 2020. URL <https://proceedings.neurips.cc/paper/2020/hash/10fb6cf4c990d2bad5ddef4f70e8ba2-Abstract.html>.
- 638
- 639 Cheng Li, Sunil Gupta, Santu Rana, Vu Nguyen, Svetha Venkatesh, and Alistair Shilton. High
 640 dimensional bayesian optimization using dropout. In Carles Sierra (ed.), *Proceedings of the
 641 Twenty-Sixth International Joint Conference on Artificial Intelligence, IJCAI 2017, Melbourne,
 642 Australia, August 19-25, 2017*, pp. 2096–2102. ijcai.org, 2017. doi: 10.24963/IJCAI.2017/291.
 643 URL <https://doi.org/10.24963/ijcai.2017/291>.
- 644
- 645 Xiaoyu Lu, Javier González, Zhenwen Dai, and Neil D. Lawrence. Structured variationally auto-
 646 encoded optimization. In Jennifer G. Dy and Andreas Krause (eds.), *Proceedings of the 35th In-
 647 ternational Conference on Machine Learning, ICML 2018, Stockholmsmässan, Stockholm, Swe-
 648 den, July 10-15, 2018*, volume 80 of *Proceedings of Machine Learning Research*, pp. 3273–3281.
 649 PMLR, 2018. URL <http://proceedings.mlr.press/v80/lu18c.html>.

- 648 Sarah Müller, Alexander von Rohr, and Sebastian Trimpe. Local policy search with bayesian op-
 649 timization. In Marc’Aurelio Ranzato, Alina Beygelzimer, Yann N. Dauphin, Percy Liang, and
 650 Jennifer Wortman Vaughan (eds.), *Advances in Neural Information Processing Systems 34: An-*
 651 *nual Conference on Neural Information Processing Systems 2021, NeurIPS 2021, December 6-*
 652 *14, 2021, virtual*, pp. 20708–20720, 2021. URL <https://proceedings.neurips.cc/paper/2021/hash/ad0f7a25211abc3889cb0f420c85e671-Abstract.html>.
- 653
- 654 Amin Nayebi, Alexander Munteanu, and Matthias Poloczek. A framework for bayesian optimization
 655 in embedded subspaces. In Kamalika Chaudhuri and Ruslan Salakhutdinov (eds.), *Proceedings*
 656 *of the 36th International Conference on Machine Learning, ICML 2019, 9-15 June 2019, Long*
 657 *Beach, California, USA*, volume 97 of *Proceedings of Machine Learning Research*, pp. 4752–
 658 4761. PMLR, 2019. URL <http://proceedings.mlr.press/v97/nayebi19a.html>.
- 659
- 660 Quan Nguyen, Kaiwen Wu, Jacob R. Gardner, and Roman Garnett. Local bayesian op-
 661 timization via maximizing probability of descent. In Sanmi Koyejo, S. Mohamed,
 662 A. Agarwal, Danielle Belgrave, K. Cho, and A. Oh (eds.), *Advances in Neural In-*
 663 *formation Processing Systems 35: Annual Conference on Neural Information Process-*
 664 *ing Systems 2022, NeurIPS 2022, New Orleans, LA, USA, November 28 - December 9,*
 665 *2022*. URL http://papers.nips.cc/paper_files/paper/2022/hash/555479a201da27c97aaeed842d16ca49-Abstract-Conference.html.
- 666
- 667 Leonard Papenmeier, Luigi Nardi, and Matthias Poloczek. Increasing the scope as you learn: Adap-
 668 tive bayesian optimization in nested subspaces. In Alice H. Oh, Alekh Agarwal, Danielle Bel-
 669 grave, and Kyunghyun Cho (eds.), *Advances in Neural Information Processing Systems*, 2022.
 670 URL <https://openreview.net/forum?id=e4Wf6112DI>.
- 671
- 672 Santu Rana, Cheng Li, Sunil Gupta, Vu Nguyen, and Svetha Venkatesh. High dimensional bayesian
 673 optimization with elastic gaussian process. In Doina Precup and Yee Whye Teh (eds.), *Pro-*
 674 *ceedings of the 34th International Conference on Machine Learning, ICML 2017, Sydney, NSW,*
 675 *Australia, 6-11 August 2017*, volume 70 of *Proceedings of Machine Learning Research*, pp. 2883–
 676 2891. PMLR, 2017. URL <http://proceedings.mlr.press/v70/rana17a.html>.
- 677
- 678 Carl Edward Rasmussen and Christopher K. I. Williams. *Gaussian processes for machine learn-*
 679 *ing*. Adaptive computation and machine learning. MIT Press, 2006. ISBN 026218253X. URL
<https://www.worldcat.org/oclc/61285753>.
- 680
- 681 Paul Rolland, Jonathan Scarlett, Ilija Bogunovic, and Volkan Cevher. High-dimensional bayesian
 682 optimization via additive models with overlapping groups. In Amos J. Storkey and Fer-
 683 nando Pérez-Cruz (eds.), *International Conference on Artificial Intelligence and Statistics, AIS-*
 684 *TATS 2018, 9-11 April 2018, Playa Blanca, Lanzarote, Canary Islands, Spain*, volume 84
 685 of *Proceedings of Machine Learning Research*, pp. 298–307. PMLR, 2018. URL <http://proceedings.mlr.press/v84/rolland18a.html>.
- 686
- 687 Kenan Sehic, Alexandre Gramfort, Joseph Salmon, and Luigi Nardi. Lassobench: A high-
 688 dimensional hyperparameter optimization benchmark suite for lasso. In Isabelle Guyon, Marius
 689 Lindauer, Mihaela van der Schaar, Frank Hutter, and Roman Garnett (eds.), *International Confer-*
 690 *ence on Automated Machine Learning, AutoML 2022, 25-27 July 2022, Johns Hopkins University,*
 691 *Baltimore, MD, USA*, volume 188 of *Proceedings of Machine Learning Research*, pp. 2/1–24.
 692 PMLR, 2022. URL <https://proceedings.mlr.press/v188/sehic22a.html>.
- 693
- 694 Yihang Shen and Carl Kingsford. Computationally efficient high-dimensional bayesian optimiza-
 695 tion via variable selection. In Aleksandra Faust, Roman Garnett, Colin White, Frank Hutter, and
 696 Jacob R. Gardner (eds.), *Proceedings of the Second International Conference on Automated Ma-*
 697 *chine Learning*, volume 224 of *Proceedings of Machine Learning Research*, pp. 15/1–27. PMLR,
 12–15 Nov 2023. URL <https://proceedings.mlr.press/v224/shen23a.html>.
- 698
- 699 Lei Song, Ke Xue, Xiaobin Huang, and Chao Qian. Monte carlo tree search based vari-
 700 able selection for high dimensional bayesian optimization. In Sanmi Koyejo, S. Mo-
 701 hamed, A. Agarwal, Danielle Belgrave, K. Cho, and A. Oh (eds.), *Advances in Neural In-*
 702 *formation Processing Systems 35: Annual Conference on Neural Information Process-*
 703 *ing Systems 2022, NeurIPS 2022, New Orleans, LA, USA, November 28 - December 9,*

- 702 2022, 2022. URL http://papers.nips.cc/paper_files/paper/2022/hash/b6a171867138c80de2a35a6125d6757c-Abstract-Conference.html.
 703
 704
- 705 Linnan Wang, Rodrigo Fonseca, and Yuandong Tian. Learning search space parti-
 706 tion for black-box optimization using monte carlo tree search. In Hugo Larochelle,
 707 Marc’Aurelio Ranzato, Raia Hadsell, Maria-Florina Balcan, and Hsuan-Tien Lin (eds.),
 708 *Advances in Neural Information Processing Systems 33: Annual Conference on Neu-*
 709 *ral Information Processing Systems 2020, NeurIPS 2020, December 6-12, 2020, vir-*
 710 *tual, 2020.* URL <https://proceedings.neurips.cc/paper/2020/hash/e2ce14e81dba66dbff9cbc35ecfdb704-Abstract.html>.
 711
- 712 Zi Wang, Chengtao Li, Stefanie Jegelka, and Pushmeet Kohli. Batched high-dimensional bayesian
 713 optimization via structural kernel learning. In Doina Precup and Yee Whye Teh (eds.), *Pro-*
 714 *ceedings of the 34th International Conference on Machine Learning, ICML 2017, Sydney, NSW,*
 715 *Australia, 6-11 August 2017*, volume 70 of *Proceedings of Machine Learning Research*, pp. 3656–
 716 3664. PMLR, 2017. URL <http://proceedings.mlr.press/v70/wang17h.html>.
 717
- 718 Ziyu Wang, Babak Shakibi, Lin Jin, and Nando de Freitas. Bayesian multi-scale optimistic op-
 719 timization. In *Proceedings of the Seventeenth International Conference on Artificial Intel-*
 720 *ligence and Statistics, AISTATS 2014, Reykjavik, Iceland, April 22-25, 2014*, volume 33 of
 721 *JMLR Workshop and Conference Proceedings*, pp. 1005–1014. JMLR.org, 2014. URL <http://proceedings.mlr.press/v33/wang14d.html>.
 722
- 723 Ziyu Wang, Frank Hutter, Masrour Zoghi, David Matheson, and Nando de Freitas. Bayesian opti-
 724 mization in a billion dimensions via random embeddings. *J. Artif. Intell. Res.*, 55:361–387, 2016.
 725 doi: 10.1613/JAIR.4806. URL <https://doi.org/10.1613/jair.4806>.
 726
- 727 Miao Zhang, Huiqi Li, and Steven W. Su. High dimensional bayesian optimization via supervised
 728 dimension reduction. In Sarit Kraus (ed.), *Proceedings of the Twenty-Eighth International Joint*
 729 *Conference on Artificial Intelligence, IJCAI 2019, Macao, China, August 10-16, 2019*, pp. 4292–
 730 4298. ijcai.org, 2019. doi: 10.24963/IJCAI.2019/596. URL <https://doi.org/10.24963/ijcai.2019/596>.
 731
- 732 Jiayu Zhao, Renyu Yang, SHENGHAO QIU, and Zheng Wang. Unleashing the potential of acqui-
 733 sition functions in high-dimensional bayesian optimization. *Transactions on Machine Learn-*
 734 *ing Research*, 2024. ISSN 2835-8856. URL <https://openreview.net/forum?id=0CM7Hfsy61>.
 735
- 736 Juliusz Krysztof Ziomek and Haitham Bou-Ammar. Are random decompositions all we need in
 737 high dimensional bayesian optimisation? In Andreas Krause, Emma Brunskill, Kyunghyun
 738 Cho, Barbara Engelhardt, Sivan Sabato, and Jonathan Scarlett (eds.), *International Confer-*
 739 *ence on Machine Learning, ICML 2023, 23-29 July 2023, Honolulu, Hawaii, USA*, volume
 740 of *Proceedings of Machine Learning Research*, pp. 43347–43368. PMLR, 2023. URL
 741 <https://proceedings.mlr.press/v202/ziomek23a.html>.
 742
 743
 744
 745
 746
 747
 748
 749
 750
 751
 752
 753
 754
 755